SÃO PAULO SCHOOL OF ADVANCED SCIENCES ON
NONLINEAR DYNAMICS
São Paulo, July 29th - August 9th, 2019

RESEARCH TOPICS ON PARAMETRIC EXCITATION

Module 29

GUILHERME ROSA FRANZINI

Escola Politécnica
University of São Paulo

SUMMARY

1. General Aspects
2. Experimental analysis of the PE of a flexible and submerged cylinder
3. Mathematical modeling of PE of a vertical and flexible cylinder
4. Passive suppression of PE

1. General Aspects
2. Experimental analysis of the PE of a flexible and submerged cylinder
3. Mathematical modeling of PE of a vertical and flexible cylinder
4. Passive suppression of PE

GENERAL ASPECTS

- Generally speaking, parametric excitation occurs when at least one of the parameters of the equations of motion explicitly depends on time;
- Focus of the lecture: The stiffness varies in time according to $k(t) = \bar{k} + \Delta k \cos(t)$;
- Classical linear problem written in the dimensionless form $\ddot{x} + (\delta + 2\epsilon \cos 2\tau)x = 0$ (undamped Mathieu's equation);
- Strutt's diagram: Straightforward way to check the stability of the trivial solution of Mathieu's equation on the plane of control parameters $(\delta; \epsilon)$. Can be either obtained using the harmonic balance method (HBM) or the method of multiple scales (MMS).

STRUTT'S DIAGRAM

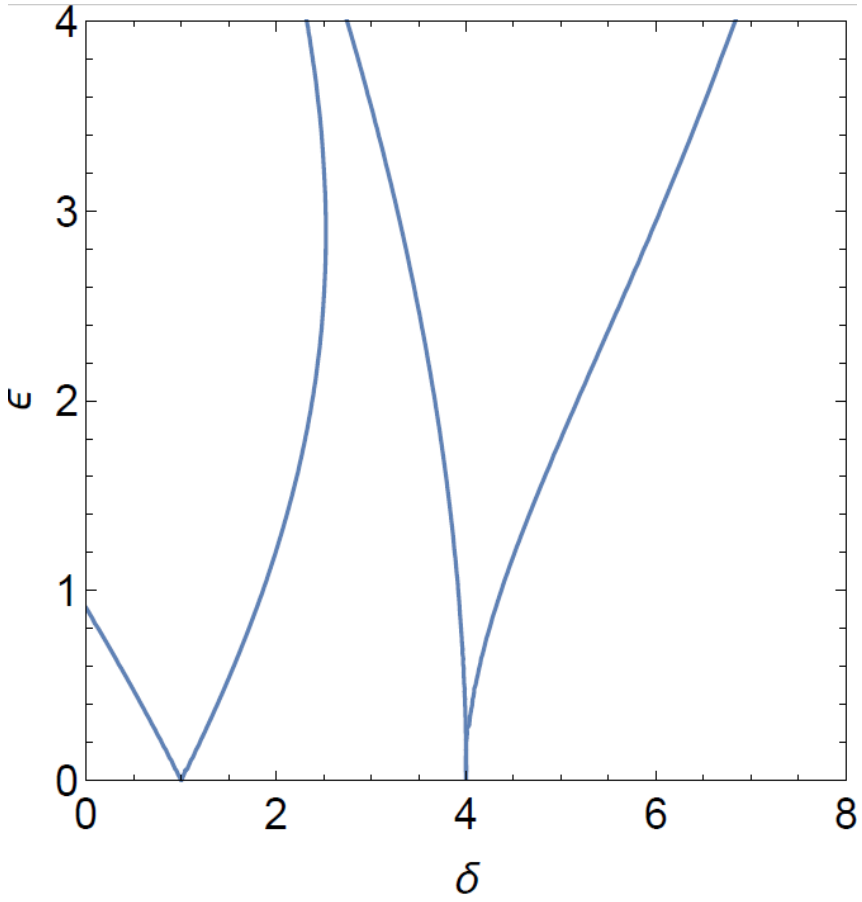

- Point located above (below) the transition curves: unbounded (bounded) solutions;
- First instability (principal parametric instability) arises at $(\delta = 1; \epsilon = 0)$. A favorable scenario for the parametric instability is that in which the parametric excitation frequency is twice the natural frequency of the system;
- Surveys on the theme: Nayfeh & Mook (1978), Meirovitch (2003) among others.

TRANSITION CURVES: DERIVATION USING THE HBM

TRANSITION CURVES: DERIVATION USING THE HBM

- Derivation valid for the undamped Mathieu's Equation: $\ddot{x} + (\delta + 2\epsilon\cos 2\tau)x = 0;$
- Using the Floquet's theory, it can be shown that the transition curves are associated with period solutions of period T or $2T$, T being the period of the parametric excitation (in our case $T = \pi$);
- We write the transition curves in the form of Fourier Series:

$$\sum_{n=0}^{\infty}\left(\tilde{a}_n\cos(n2\tau) + \tilde{b}_n\sin(n2\tau)\right) + \sum_{n=0}^{\infty}\left(\tilde{c}_n\cos(n\tau) + \tilde{d}_n\sin(n\tau)\right) = \sum_{n=0}^{\infty}\left(a_n\cos(n\tau) + b_n\sin(n\tau)\right)$$

TRANSITION CURVES: DERIVATION USING THE HBM

- Some useful mathematical identities

$$\cos(2\tau)\cos(n\tau) = \left(\frac{e^{i2\tau}+e^{-i2\tau}}{2}\right)\left(\frac{e^{in\tau}+e^{-in\tau}}{2}\right) = \frac{1}{2}\cos\big((2+n)\tau\big) + \frac{1}{2}\cos((2-n)\,\tau)$$

$$\cos(2\tau)\sin(n\tau) = \left(\frac{e^{i2\tau}+e^{-i2\tau}}{2}\right)\left(\frac{e^{in\tau}-e^{-in\tau}}{2i}\right) = \frac{1}{2}\sin\big((2+n)\tau\big) + \frac{1}{2}\sin((n-2)\,\tau))$$

$$xcos(2\tau) = \sum_{n=0}^{\infty}\left[a_n\left(\frac{1}{2}\cos\big((2+n)\tau\big) + \frac{1}{2}\sin((2-n)\,\tau)\right) + b_n\left(\frac{1}{2}\sin\big((2+n)\tau\big) + \frac{1}{2}\sin((n-2)\,\tau))\right)\right]$$

$$\ddot{x} = -\sum_{n=0}^{\infty} n^2(a_n\cos(n\tau) + b_n\sin(n\tau))$$

TRANSITION CURVES: DERIVATION USING THE HBM

- Expansion using three terms in the Fourier Series:
- $\delta x = \delta a_0 + \delta a_1 cos\tau + \delta b_1 sin\tau + \delta a_2 cos\, 2\tau + \delta b_2 sin2\tau$
- $xcos(2\tau) = \frac{a_0}{2}(cos2\tau + cos2\tau) + \frac{a_1}{2}(cos3\tau + cos\tau) + \frac{b_1}{2}(sin3\tau - sin\tau) + \frac{a_2}{2}(\cos 4\tau + 1) + \frac{b_2}{2} sin4\tau$
- $\ddot{x} = -(a_1 cos\tau + b_1 sin\tau + 4a_2 cos2\tau + 4b_2 sin2\tau)$

Substituting the above quantities into the Mathieu's equation, one obtains:

$$(-a_1 + \delta a_1 + \epsilon a_1)cos\tau + (-b_1 + \delta b_1 - \epsilon b_1)sin\tau + (-4a_2 + \delta a_2 + 2\epsilon a_0)cos2\tau + (-4b_2 + \delta b_2)sin2\tau + (\dots) = 0$$

(...) being higher-order harmonics not considered in the expansion.

TRANSITION CURVES: DERIVATION USING THE HBM

- As the trigonometric functions are orthogonal according to the usual inner product:

$$\begin{pmatrix} 0 & -1+\delta+\epsilon & 0 & 0 & 0 \\ 0 & 0 & -1+\delta+\epsilon & 0 & 0 \\ 2\epsilon & 0 & 0 & -4+\delta & 0 \\ 0 & 0 & 0 & 0 & -4+\delta \\ \delta & 0 & 0 & \epsilon & 0 \end{pmatrix} \begin{Bmatrix} a_0 \\ a_1 \\ b_1 \\ a_2 \\ b_2 \end{Bmatrix} = \begin{Bmatrix} 0 \\ 0 \\ 0 \\ 0 \\ 0 \end{Bmatrix}$$

- Non-trivial solutions of the above equations exist if the determinant of the coefficients matrix is null, i.e., if

$$(4\delta - \delta^2 + 2\epsilon^2)(-4+\delta)(-1+\delta-\epsilon)(-1+\delta+\epsilon) = 0$$

TRANSITION CURVES: DERIVATION USING THE HBM

- The description of the Strutt's diagram is improved if more terms are considered in the HBM. Symbolic computation is a valuable tool here.

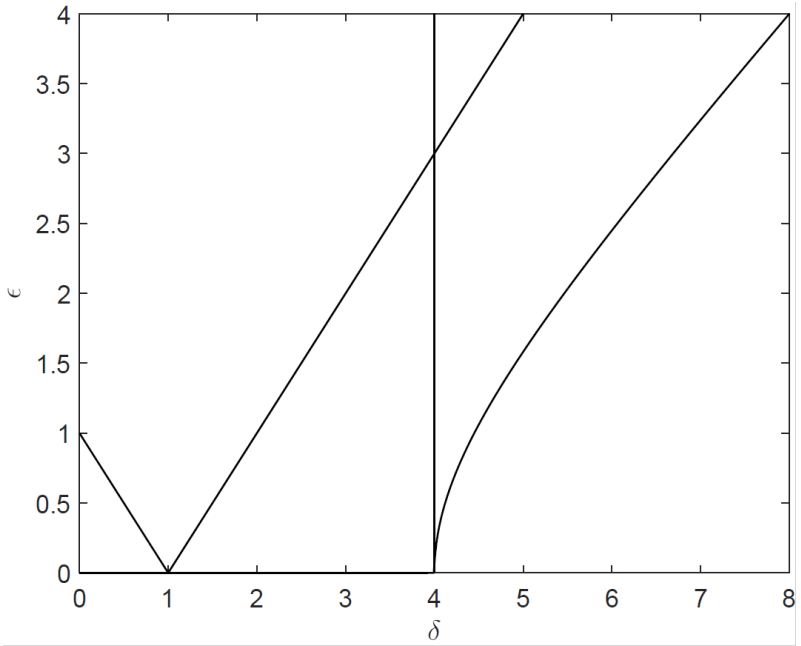

- 3 terms

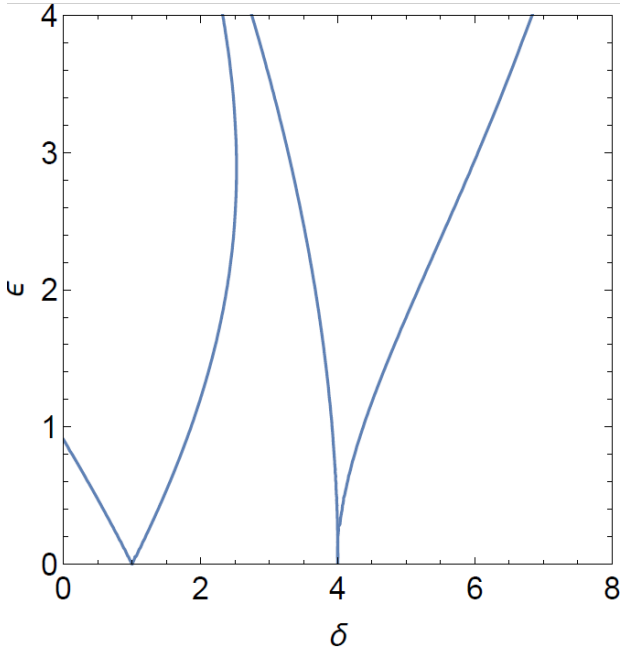

- 7 terms

TRANSITION CURVES: DERIVATION USING THE MMS

TRANSITION CURVES: DERIVATION USING THE MMS

- Derivation presented in Nayfeh (1978) – Perturbation methods
- Mathieu's equations written in the form: $\ddot{u} + (\delta + \epsilon \cos(2\tau))u = 0;$
- Notice that $\delta = \omega_0^2, \omega_0$ being the natural frequency of the oscillator;

- Following the MMS, different time-scales are defined as $\tau_n = \epsilon^n \tau;$
- Solution is sought on the form:

$$u = u_0 + \epsilon u_1 + \epsilon^2 u_2$$

with $u_j = u_j(\tau_0, \tau_1, \tau_2), j = 0,1$ and 2

- Family of differential operators: $D_n^k( ) = \frac{\partial^k}{\partial \tau_n^k}( )$

TRANSITION CURVES: DERIVATION USING THE MMS

$$\dot{(\,)} = \frac{d(\,)}{d\tau} = \frac{d(\,)}{d\tau_0}\frac{d\tau_0}{d\tau} + \frac{d(\,)}{d\tau_1}\frac{d\tau_1}{d\tau} + \frac{d(\,)}{d\tau_2}\frac{d\tau_2}{d\tau} = (D_0 + \epsilon D_1 + \epsilon^2 D_2)(\,) + O(\epsilon^3)$$

$$\ddot{(\,)} = \frac{d^2(\,)}{d\tau^2} = (D_0 + \epsilon D_1 + \epsilon^2 D_2)(D_0 + \epsilon D_1 + \epsilon^2 D_2)(\,) = (D_0^2 + \epsilon 2 D_0 D_1 + \epsilon^2 (2 D_0 D_2 + D_1^2))(\,) + O(\epsilon^3)$$

Focus of this class: Principal Mathieu's instability $(\delta = 1) \rightarrow \delta = 1 + \epsilon\delta_1 + \epsilon^2\delta_2 + O(\epsilon^3)$

Using the above definitions, the terms of the Mathieu's equation read

$$\ddot{u} = (D_0^2 + \epsilon 2 D_0 D_1 + \epsilon^2 (2 D_0 D_2 + D_1^2))(u_0 + \epsilon u_1 + \epsilon^2 u_2) =$$
$$= D_0^2 u_0 + \epsilon (D_0^2 u_1 + 2 D_0 D_1 u_0) + \epsilon^2 (D_1^2 u_0 + 2 D_0 D_2 u_0 + D_0^2 u_2 + 2 D_0 D_1 u_1) + O(\epsilon^3)$$

$$\epsilon \cos(2\tau)\, u = \epsilon \cos(2\tau_0)\,(u_0 + \epsilon u_1 + \epsilon^2 u_2) = \epsilon u_0 \cos(2\tau_0) + \epsilon^2 u_1 \cos(2\tau_0) + O(\epsilon^3)$$

$$\delta u = (1 + \epsilon\delta_1 + \epsilon^2\delta_2)(u_0 + \epsilon u_1 + \epsilon^2 u_2) = u_0 + \epsilon(\delta_1 u_0 + u_1) + \epsilon^2 (u_2 + \delta_2 u_0 + \delta_1 u_1) + O(\epsilon^3)$$

TRANSITION CURVES: DERIVATION USING THE MMS

By substituting $\ddot{u}, \epsilon \cos(2\tau)\, u$ and δu in the Mathieu's equation and collecting terms of equal power in ϵ, one obtains:

$$O(\epsilon^0):\ D_0^2 u_0 + u_0 = 0$$
$$O(\epsilon):\ D_0^2 u_1 + u_1 = -u_0 \cos(2\tau_0) - \delta_1 u_0 - 2D_1 D_0 u_0$$
$$O(\epsilon^2):\ D_0^2 u_2 + u_2 = -\delta_2 u_0 - \delta_1 u_1 - u_1 \cos(2\tau_0) - D_1^2 u_0 - 2D_0 D_2 u_0 - 2D_0 D_1 u_1$$

The application of the MMS leads to a series of linear equations in which the solutions of the faster scales "force" the lower ones.

Solution of the equation of order ϵ^0: $u_0 = Ae^{i\tau_0} + A^* e^{-i\tau_0} = Ae^{i\tau_0} + c.c;\ \ A = A(\tau_1, \tau_2)$ being a complex amplitude.

Useful identities: $D_0 u_0 = iAe^{i\tau_0} - iA^* e^{-i\tau_0} = iAe^{i\tau_0} + c.c.$

$$D_1 D_0 u_0 = iD_1 Ae^{i\tau_0} + c.c.$$

$$u_0 \cos(2\tau_0) = \left(Ae^{i\tau_0} + A^* e^{-i\tau_0}\right)\left(\frac{e^{i2\tau_0} + e^{-i2\tau_0}}{2}\right) = \frac{1}{2}\left(Ae^{i3\tau_0} + A^* e^{i\tau_0}\right) + c.c.$$

TRANSITION CURVES: DERIVATION USING THE MMS

Substituting these identities into the equation of order $O(\epsilon)$:

$$D_0^2 u_1 + u_1 = -\frac{1}{2} A e^{i3\tau_0} + \underbrace{\left(-\frac{1}{2} A^* - \delta_1 A - i2D_1 A\right) e^{i\tau_0}}_{\text{Resonant term}} + c.c.$$

Resonant terms give rise to secular terms (unbounded solutions) and must be removed.

Solvability condition: $$\left(-\frac{1}{2} A^* - \delta_1 A - i2D_1 A\right) = 0 \leftrightarrow D_1 A = \frac{i}{2}\left(\delta_1 A + \frac{1}{2} A^*\right)$$

TRANSITION CURVES: DERIVATION USING THE MMS

$$A = a + ib \rightarrow A^* = a - ib, a, b \text{ real numbers}$$

$$D_1 A = \frac{i}{2}\left(\delta_1 A + \frac{1}{2}A^*\right) \rightarrow D_1 a + iD_1 b = \frac{i}{2}\left(\left[\delta_1 + \frac{1}{2}\right]a + i\left[\delta_1 - \frac{1}{2}\right]b\right)$$

Separating into real and imaginary parts:

$$D_1 a = \frac{1}{2}\left(\frac{1}{2} - \delta_1\right)b$$

$$D_1 b = \frac{1}{2}\left(\frac{1}{2} + \delta_1\right)a$$

→

First-order system of autonomous differential equations:
Stability can be studied using the first Lyapunov's method.

TRANSITION CURVES: DERIVATION USING THE MMS

$$\begin{Bmatrix} D_1 a \\ D_1 b \end{Bmatrix} = \begin{bmatrix} 0 & \frac{1}{2}\left(\frac{1}{2} - \delta_1\right) \\ \frac{1}{2}\left(\frac{1}{2} + \delta_1\right) & 0 \end{bmatrix} \begin{Bmatrix} a \\ b \end{Bmatrix}$$

Solutions are sought in the form $\begin{Bmatrix} a \\ b \end{Bmatrix} = \tilde{\boldsymbol{A}} e^{\lambda t}$. The existence of non-trivial solutions implies that

$$det \begin{bmatrix} -\lambda & \frac{1}{2}\left(\frac{1}{2} - \delta_1\right) \\ \frac{1}{2}\left(\frac{1}{2} + \delta_1\right) & -\lambda \end{bmatrix} = \lambda^2 - \frac{1}{4}\left(\frac{1}{4} - \delta_1^2\right) = 0 \rightarrow \lambda = \pm\frac{1}{2}\sqrt{\left(\frac{1}{4} - \delta_1^2\right)}$$

TRANSITION CURVES: DERIVATION USING THE MMS

$$\lambda = \pm\frac{1}{2}\sqrt{\left(\frac{1}{4} - \delta_1^2\right)}$$

- Case 1: $-\frac{1}{2} < \delta_1 < \frac{1}{2} \rightarrow \lambda = \frac{1}{2}\sqrt{\frac{1}{4} - \delta_1^2} > 0$ (unbounded solution)
- Case 2: $\delta_1 > \frac{1}{2}$ and $\delta_1 < -\frac{1}{2} \rightarrow \lambda = \pm\frac{i}{2}\sqrt{\delta_1^2 - \frac{1}{4}}$ (bounded solution)
- Case 3: $\delta_1 = \pm\frac{1}{2}$ (transition curves)

Recalling that $\delta = 1 + \epsilon\delta_1 + O(\epsilon^2)$, the transition curves are defined as $\delta = 1 + \frac{\epsilon}{2}$ or $\delta = 1 - \frac{\epsilon}{2}$. In an equivalently manner, $\epsilon = 2(\delta - 1)$ or $\epsilon = 2(-\delta + 1)$.

TRANSITION CURVES: DERIVATION USING THE MMS

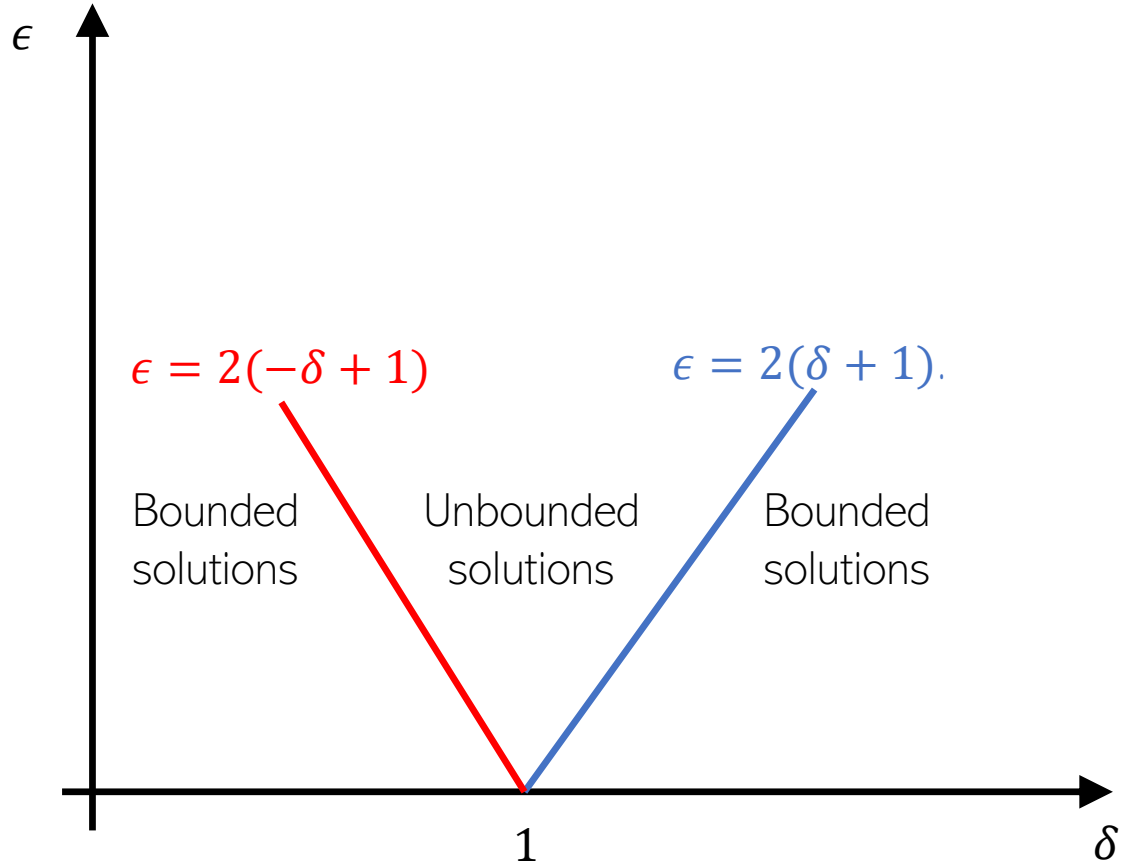

TECHNOLOGICAL IMPORTANCE

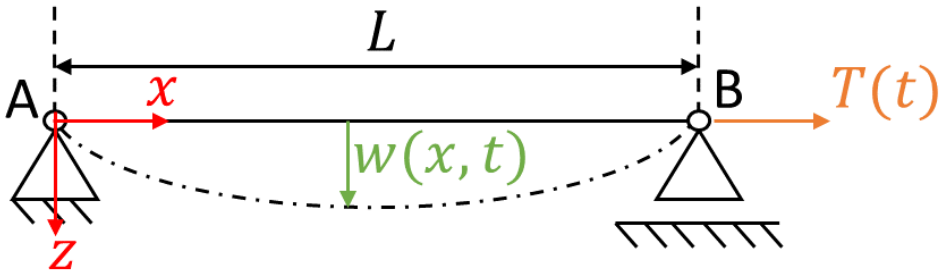

- Cables have their lateral stiffness associated with the normal force (geometric stiness);
- Tension depends on time → geometric stiffness also depends on it;
- In offshore scenario, slender structures such as risers and TLP's tethers, the motion of the floating units on the vertical plane induces a time-dependent tension;
- May be important due to structural fatigue.

AN OVERVIEW ON RISERS DYNAMICS

- Focus on the oshore scenario Patel & Park (1991): Effects of the quadratic damping (Morrison's equation) is taken into account on the reduced-order models (ROMs) → Bounded solutions are obtained even in the region in which the Strutt's diagram predicts unbounded responses;
- Simos & Pesce (1997) and Chandrasekaran et al. (2006): The spatial variation of tension may be of importance on the study of the parametric instability;
- The aforementioned papers deal with the case in which the tension harmonically varies with respect to time → Some aspects of the irregular parametric excitation in risers can be found in the numerical paper by Yang, Xiao and Xu (2013).

RESEARCH OPPORTUNITIES

- Experimental investigations focusing on the parametric excitation of submerged cylinders;
- Numerical studies focusing on the post-critical response (i.e, after the parametric instability);
- Experimental studies focusing on the response of a flexible cylinder to irregular parametric excitation.

1. General Aspects
2. Experimental analysis of the PE of a flexible and submerged cylinder
3. Mathematical modeling of PE of a vertical and flexible cylinder
4. Passive suppression of PE

CONTEXTUALIZATION

- Focus: PE of a flexible and submerged vertical cylinder;
- Experiments carried out at Technological Research Institute (IPT-SP) as part of a comprehensive project sponsored by Petrobras (2009-2013);
- Innovative aspects of the experimental set-up: Cartesian coordinates of 43 reflective targets were directly measured by means of an optical tracking system (Qualisys®) – uncertainty lower than $\mathbf{0.1}$mm
- VIV is obtained by towing the carriage in which the model is assembled. PE is achieved by using a servomotor device for imposing a vertical and harmonic top motion with amplitude A_t and frequency f_t . Temporal variation of the normal force (geometric stiffness modulation).

EXPERIMENTAL ARRANGEMENT

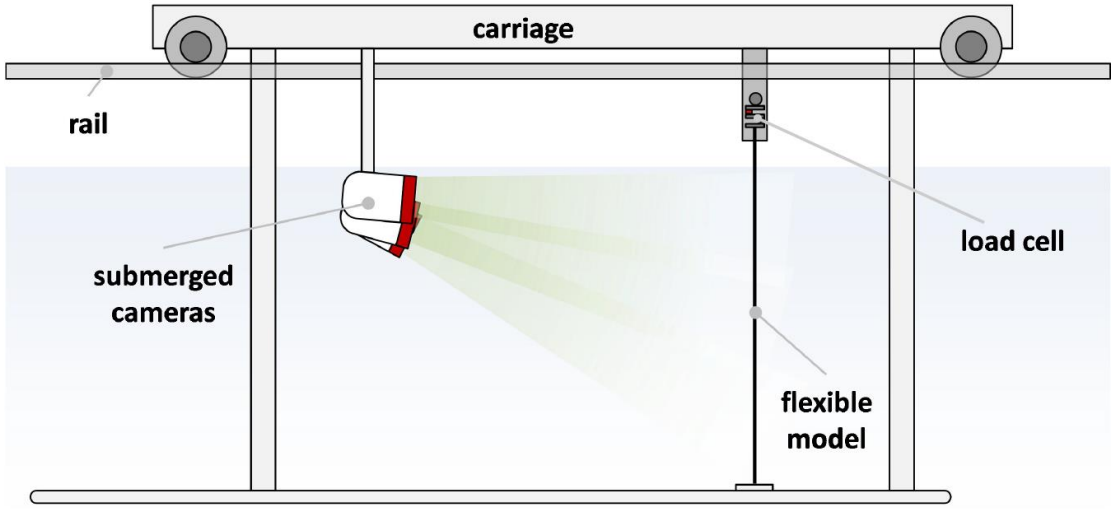

(a) Lateral view.

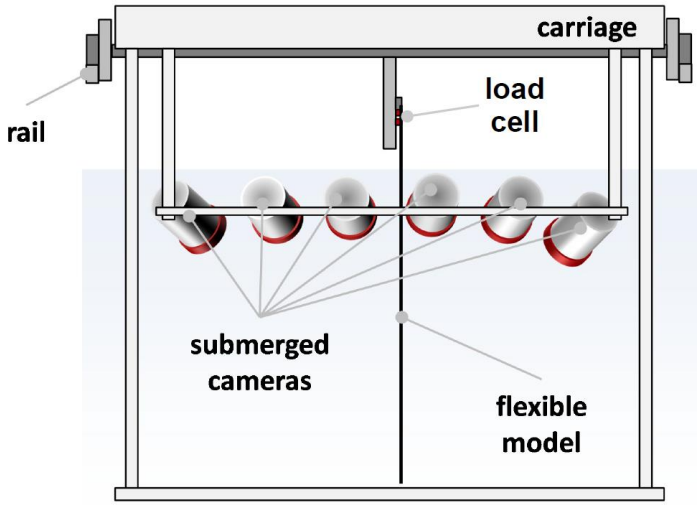

(b) Back view.

Extracted from Franzini et al. (2016a).

EXPERIMENTAL ARRANGEMENT AND CYLINDRICAL MODEL

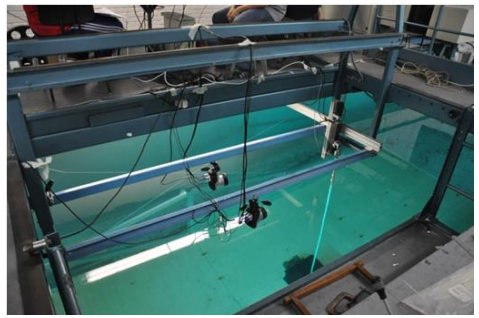

(a) General view.

(b) Submerged cameras.

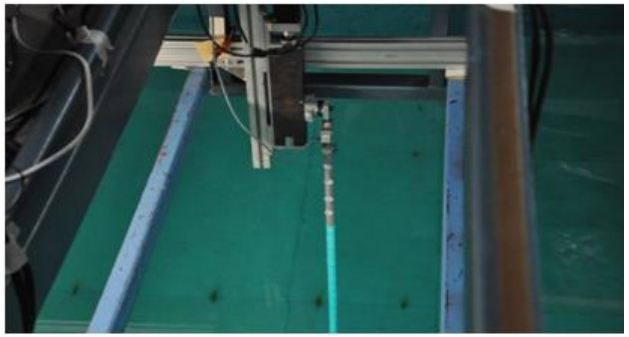

(c) Servomotor device.

Extracted from Franzini et al. (2015).

Property		
External diameter D		22.2 mm
Axial stiffness EA		1.2 kN
Bending stiffness EI		0.056 Nm^2
Linear mass m_l		1.19 kg/m
Immersed weight γ		7.88 N/m
Unstretched length L_0		2552 mm
Stretched length L		2602 mm
Immersed length L_i		2257 mm
Mass ratio parameter m^*		3.48
Aspect ratio L_i/D		102
L/D		117
Static tension at the top T_t		40 N
ζ_1		4.17%
ζ_1^{ar}		0.49%
Natural frequencies		
mode k	$f_{n,k}^{air}$	$f_{n,k}$
1	1.00 Hz	0.84 Hz
2	2.05 Hz	1.68 Hz
3	3.10 Hz	2.52 Hz

Extracted from Franzini et al. (2018).

EXPERIMENTAL MODAL ANALYSIS

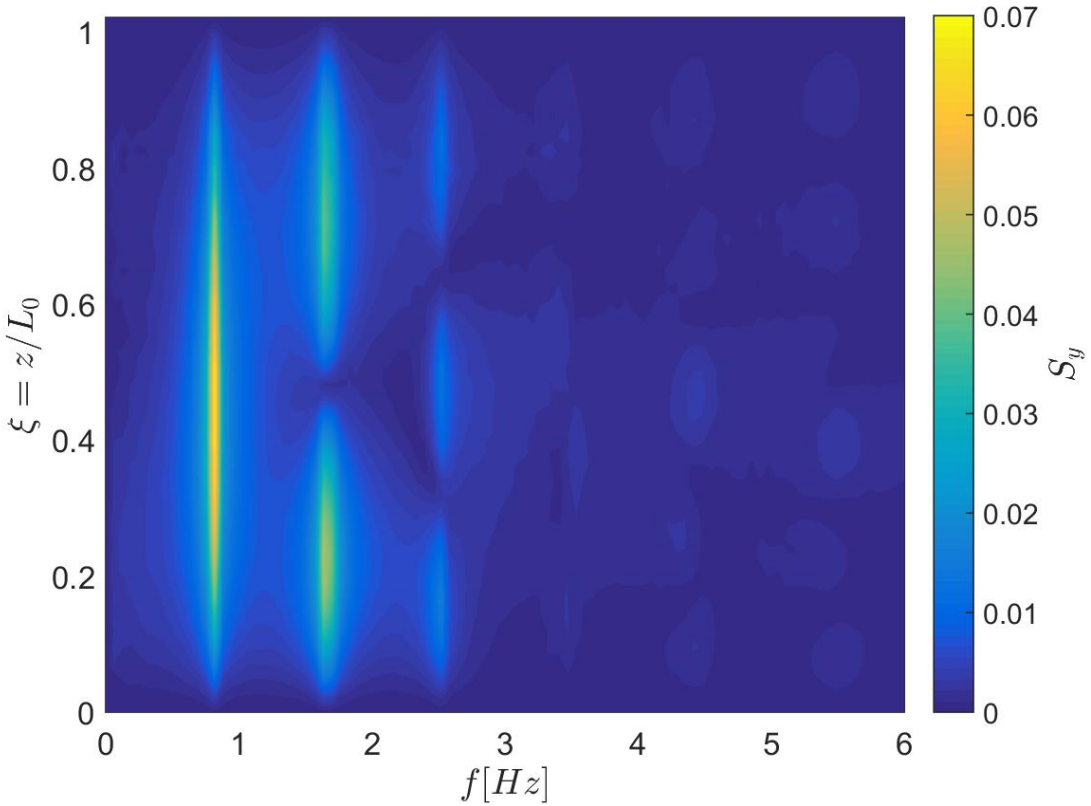

Adapted from Franzini et al. (2015).

ANALYSIS METHODOLOGIES

- Standard techniques: Based on the time-histories of each monitored target; statistics and amplitude spectra;
- Modal decomposition scheme: Projection of the measured response onto a set of "modal functions" $\psi_k(\xi) = \sin(k\pi\xi)$.

Trigonometric functions are not the vibration modes for a vertical rod

$$\tilde{a}_k^x(t_j) = \frac{\int_0^1 X^*(\xi,t_j)\psi_k(\xi)d\xi}{\int_0^1(\psi_k(\xi))^2 d\xi} \quad (1)$$

$$\tilde{a}_k^y(t_j) = \frac{\int_0^1 Y^*(\xi,t_j)\psi_k(\xi)d\xi}{\int_0^1(\psi_k(\xi))^2 d\xi} \quad (2)$$

$$\xi = z/L_0$$

PE OF A VERTICAL AND FLEXIBLE CYLINDER

- Published in Franzini et al. (2015) - J. Vib. Acoustics, v.137(3), 031010-1 - 031010-12. ResearchGate project named Risers Mechanics;
- Experimental investigations on the PE of a submerged cylinder are not commonly found;
- Cases to be discussed: $f_t: f_{n,1} = 1:3, f_t: f_{n,1} = 1:1, f_t: f_{n,1} = 2:1 \; and \; f_t: f_{n,1} = 3:1, all \; with \; A_t = L_0 = 0{:}01.$
- For the sake of conciseness of this presentation, the modal-amplitude time-histories are discussed.
- Modal form of the equation of motion (after the application of the Galerkin's method considering a unimodal projection):

$$M_k \frac{d^2 a_k}{dt^2} + \beta_k \left|\frac{da_k}{dt}\right| \frac{da_k}{dt} + \left(\eta_k + \xi_k \cos(\omega_t t)\right) a_k = 0 \qquad (3)$$

PE OF A VERTICAL AND FLEXIBLE CYLINDER

$$M_k = \int_0^{L_0} m_t \psi_k^2(z)\, dz = \left(m_I + m_a^{pot}\right)\frac{L_0}{2} \tag{4}$$

$$\beta_k = \int_0^{L_0} \frac{1}{2}\rho C_D D |\psi_k(z)| \psi_k^2(z) dz \tag{5}$$

$$\eta_k = -\int_0^{L_0} \frac{\partial}{\partial_z}\left[\left(T_t - \gamma(L_0 - z)\right)\frac{d\psi(z)}{dz}\right]\psi_k(z) dz = \left(\frac{k\pi}{2}\right)^2 \left(2\,\frac{T_t}{L_0} - \gamma\right) \tag{6}$$

$$\xi_k = \left(\frac{k\pi}{2}\right)^2 \left(\frac{EA}{L_0}\right)\frac{2\,A_t}{L_0} \tag{7}$$

Dimensionless mathematical model:

$$\ddot{\tilde{a}} + 2\mu_k\, D\dot{\tilde{a}}_k|\dot{\tilde{a}}_k| + (\delta_k + 2\epsilon_k \cos(2\tau))\tilde{a}_k = 0 \tag{8}$$

$$2\tau = \omega_t t = 2\pi f_t t, \mu_k = \frac{\beta_k}{2M_K}, \delta_K = \frac{4n_k}{M_k\omega_t^2}, \epsilon_k = \frac{2\xi_k}{M_k\omega_t^2} \tag{9}$$

PE: MODAL STRUTT'S DIAGRAMS

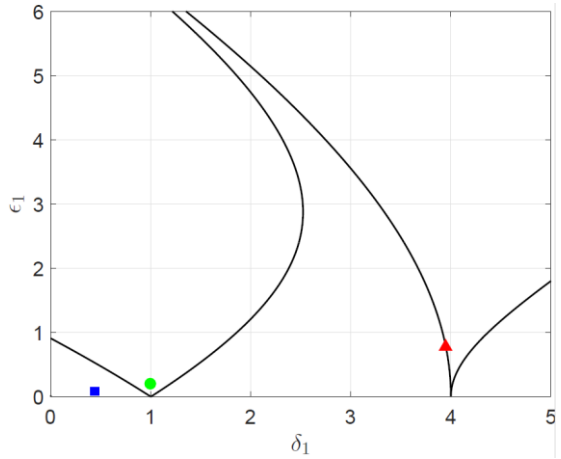

(a) $k = 1$

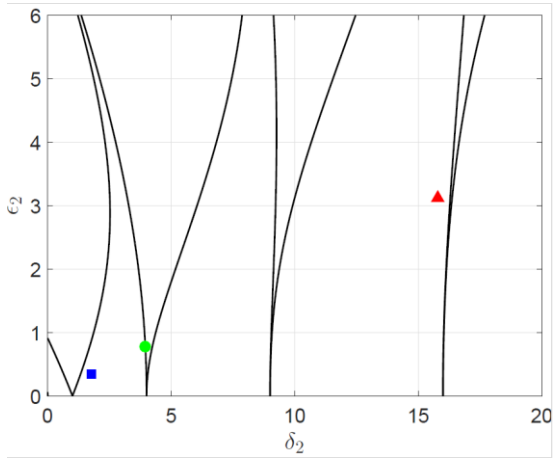

(b) $k = 2$

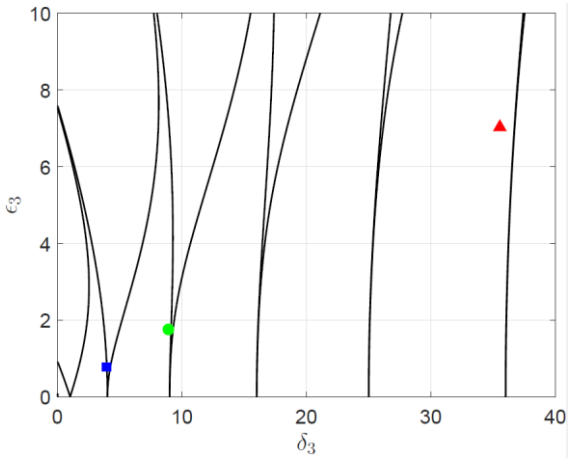

(c) $k = 3$

Adapted from Franzini et al. (2015)

▲ $f_t : f_{n,1} = 1:1$

● $f_t : f_{n,1} = 1:2$

■ $f_t : f_{n,1} = 3:1$

The marker for the case $f_t : f_{n,1} = 1:3$ is inside the stable region and is not visible in the adopted scale.

PE: MODAL-AMPLITUDE TIME-HISTORIES - $\tilde{a}_1(\tau)$

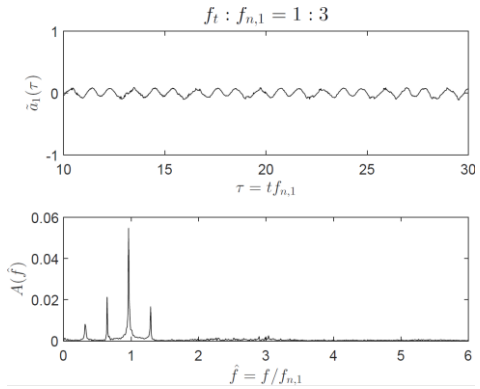

(a) f_t: $f_{n,1} = 1:3$

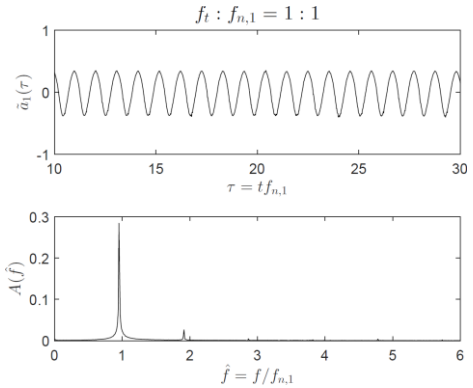

(b) f_t : $f_{n,1} = 1:1$

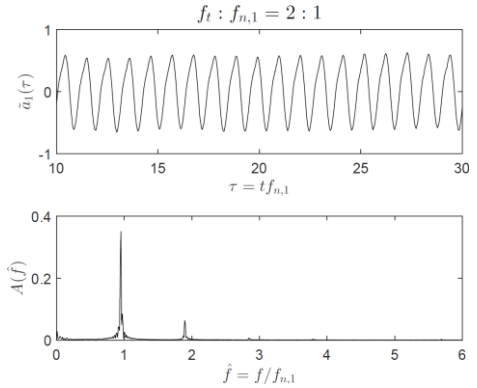

(c) f_t : $f_{n,1} = 2:1$

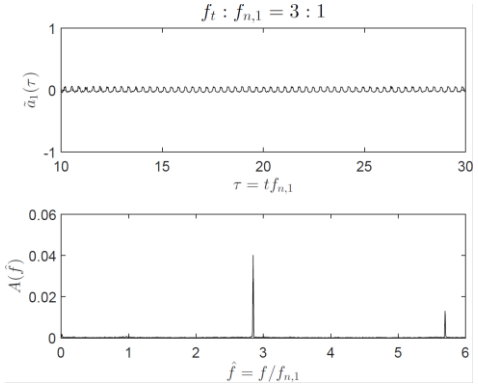

(d) f_t : $f_{n,1} = 3:1$

Adapted from Franzini et al. (2015).

Significant responses in the first mode for the cases:

- f_t : $f_{n,1} = 1:1$ (classical resonance);
- f_t : $f_{n,1} = 2:1$ (principal parametric instability of the first mode).

PE: MODAL-AMPLITUDE TIME-HISTORIES - $\tilde{a}_2(\tau)$

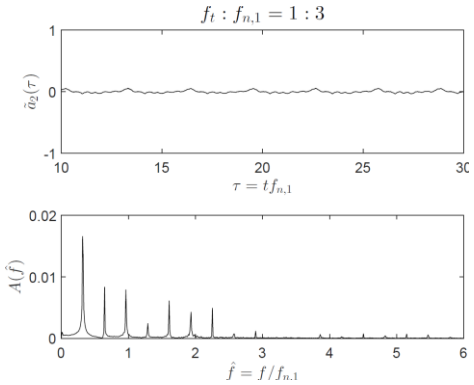

(a) f_t: $f_{n,1} = 1:3$

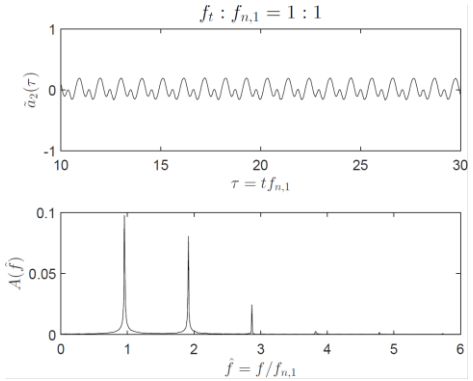

(b) $f_t : f_{n,1} = 1:1$

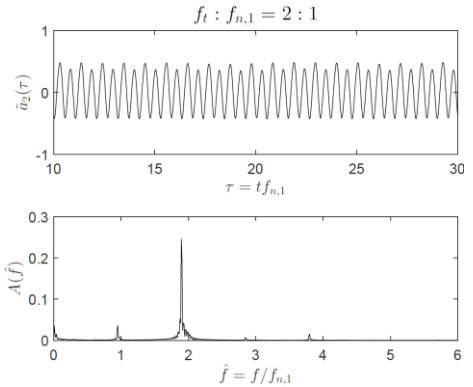

(c) $f_t : f_{n,1} = 2:1$

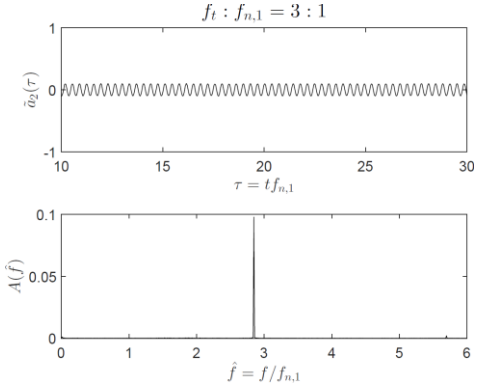

(d) $f_t : f_{n,1} = 3:1$

Adapted from Franzini et al. (2015).

Significant responses in the second mode for the cases:

- $f_t : f_{n,1} = 2:1$ (classical resonance);
- $f_t : f_{n,1} = 3:1 \rightarrow$ responses with the shape of the second mode with frequency close to $f_{n,3}$.

PE: MODAL-AMPLITUDE TIME-HISTORIES - $\tilde{a}_3(\tau)$

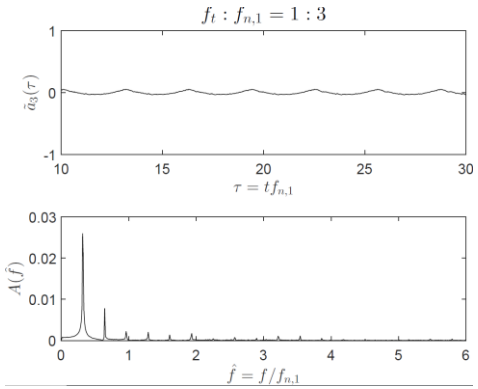

(a) f_t: $f_{n,1} = 1 : 3$

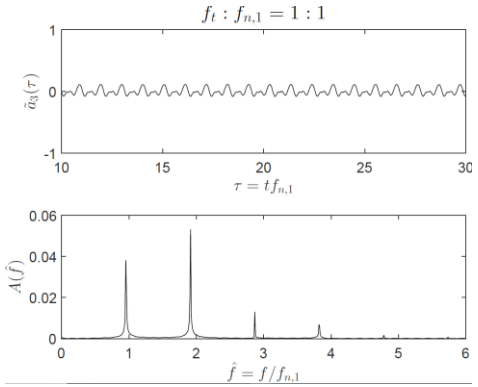

(b) f_t : $f_{n,1} = 1 : 1$

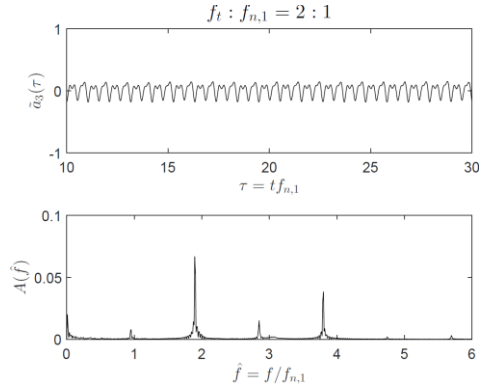

(c) f_t : $f_{n,1} = 2 : 1$

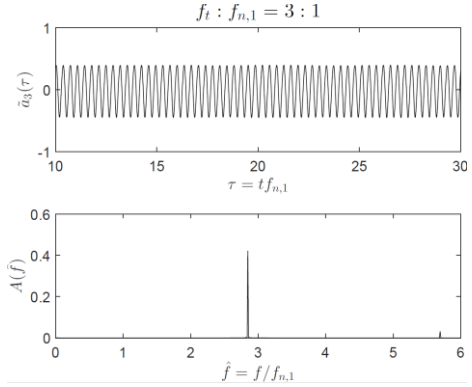

(d) f_t : $f_{n,1} = 3 : 1$

Adapted from Franzini et al. (2015).

Significant responses in the third mode for the case:

- f_t : $f_{n,1} = 3 : 1$ (classical resonance).

1. General Aspects
2. Experimental analysis of the PE of a flexible and submerged cylinder
3. Mathematical modeling of PE of a vertical and flexible cylinder
4. Passive suppression of PE

PARAMETRIC EXCITATION OF A VERTICAL AND IMMERSED CYLINDER

- Start-point: Non-linear equations of motion for the planar dynamics of a vertical cylinder (see Mazzilli et al. (2008).
- Contribution: Analysis oh the parametric excitation of a vertical and immersed flexible cylinder using a multi-modal ROM.
- Rom obtained by applying the Galerkin's method on the equations of motion for the continuum.
- Results published in Franzini & Mazzilli (2016), Int. J. of Non-Linear Mech., v.80,29-39.

SKETCHES AND MATHEMATICAL MODEL FOR THE CONTINUUM

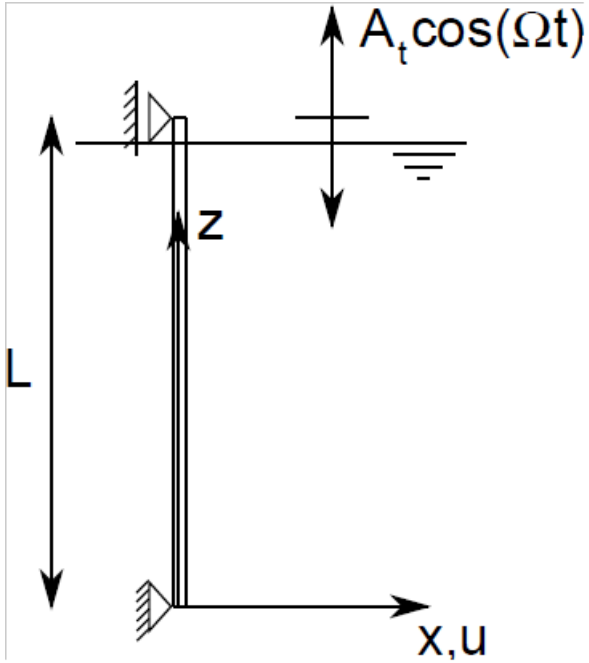

(a) Vertical and stretched cylinder

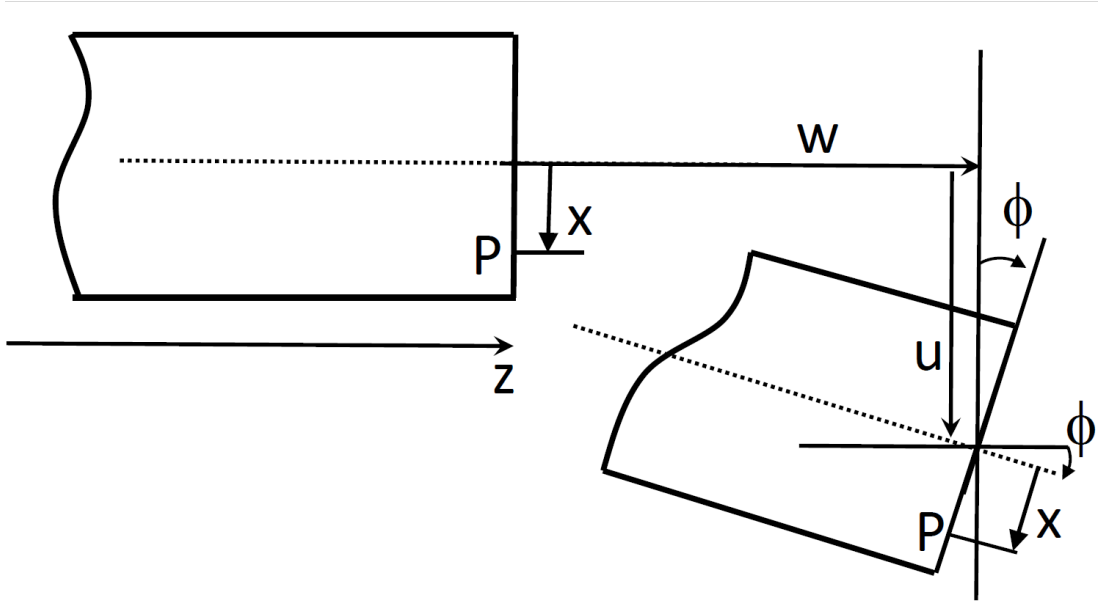

(b) Kinematical hyphothesis.

SKETCHES AND MATHEMATICAL MODEL FOR THE CONTINUUM

$$m_l \frac{\partial^2 u}{\partial t^2} + c\frac{\partial u}{\partial t} + EI\frac{\partial^4 u}{\partial z^4} - \frac{\partial}{\partial z}\left(T\,(z,t)\frac{\partial u}{\partial z}\right) - \frac{EA}{2L_0}\frac{\partial^2 u}{\partial z^2}\int_0^{L_0}\left(\frac{\partial u}{\partial z}\right)^2 dz = -m_a^{pot}\frac{\partial^2 u}{\partial t^2} - \frac{1}{2}\rho D\bar{C}_D\left|\frac{\partial u}{\partial t}\right|\frac{\partial u}{\partial t}$$

Non-linear equation of motion for the continuum: immersed cylinder

$$T(z,t) = -\gamma(L_0 - z) + \underbrace{\bar{T}_t + \frac{EA}{L_0}A_t\,(\cos\Omega t)}_{T_t(t)}$$

$$u(z,t) = \sum_{k=1}^{3}\psi_k(z)\,a_k(t); \frac{du(z,t)}{dt} = \sum_{k=1}^{3}\psi_k(z)\frac{da_k(t)}{dt}$$

$$\frac{d^2u(z,t)}{dt^2} = \sum_{k=1}^{3}\psi_k(z)\frac{d^2a_k(z)}{dt^2}; \frac{du(z,t)}{dz} = \sum_{k=1}^{3}\frac{d\psi_k(z)}{dz}a_k(t)$$

$$\frac{d^2u(z,t)}{dz^2} = \sum_{k=1}^{3}\frac{d^2\psi_k(z)}{dz^2}a_k(t); \frac{d^4u(z,t)}{dz^4} = \sum_{k=1}^{3}\frac{d^4\psi_k(z)}{dz^4}a_k(t)$$

DIMENSIONLESS ROM

Dimensionless quantities

$$\tau = t\omega_{n,1}; \xi = \frac{z}{L_0} n = \frac{\Omega}{\omega_{n,1}}; \tilde{a}_k = \frac{a_k}{D}; C_a^{pot} = \frac{m_a^{pot}}{m_d}; \tilde{m} = \frac{m_I}{M_D} \Lambda_M = \frac{D^2}{m_d\left(\tilde{m} + C_a^{pot}\right)} \rho \bar{C}_D$$

Multi-modal ROM (after the application of the Galerkin´s method)

$$\ddot{\tilde{a}}_1 + \alpha_1 \dot{\tilde{a}}_1 + (\delta_1 + \epsilon_1 \cos(n\tau))\tilde{a}_1 + \alpha_2 \tilde{a}_2 + \alpha_3 \tilde{a}_1^3 + \alpha_4 \tilde{a}_2^2 \tilde{a}_1 + \alpha_5 \tilde{a}_1 \tilde{a}_3^2 + \Lambda_M \int_0^1 \left|\dot{\tilde{a}}_1 \psi_1 + \dot{\tilde{a}}_2 \psi_2 + \dot{\tilde{a}}_3 \psi_3\right| \left(\dot{\tilde{a}}_1 \psi_1 + \dot{\tilde{a}}_2 \psi_2 + \dot{\tilde{a}}_3 \psi_3\right) \psi_1 d\xi = 0$$

$$\ddot{\tilde{a}}_2 + \beta_1 \dot{\tilde{a}}_2 + (\delta_2 + \epsilon_2 \cos(n\tau))\tilde{a}_2 + \beta_2 \tilde{a}_3 + \beta_3 \tilde{a}_1 + \beta_4 \tilde{a}_2 \tilde{a}_1^2 + \beta_5 \tilde{a}_2^3 + \beta_6 \tilde{a}_{\,2} \tilde{a}_3^2 + \Lambda_M \int_0^1 \left|\dot{\tilde{a}}_1 \psi_1 + \dot{\tilde{a}}_2 \psi_2 + \dot{\tilde{a}}_3 \psi_3\right| \left(\dot{\tilde{a}}_1 \psi_1 + \dot{\tilde{a}}_2 \psi_2 + \dot{\tilde{a}}_3 \psi_3\right) \psi_2 d\xi = 0$$

$$\ddot{\tilde{a}}_3 + \gamma_1 \dot{\tilde{a}}_3 + (\delta_3 + \epsilon_3 \cos(n\tau))\tilde{a}_3 + \gamma_2 \tilde{a}_2 + \gamma_3 \tilde{a}_3 \tilde{a}_2^2 + \gamma_4 \tilde{a}_3 \tilde{a}_1^2 + \gamma_5 \tilde{a}_3^3 + \Lambda_M \int_0^1 \left|\dot{\tilde{a}}_1 \psi_1 + \dot{\tilde{a}}_2 \psi_2 + \dot{\tilde{a}}_3 \psi_3\right| \left(\dot{\tilde{a}}_1 \psi_{\,1} + \dot{\tilde{a}}_2 \psi_2 + \dot{\tilde{a}}_3 \psi_3\right) \psi_3 d\xi = 0$$

DIMENSIONLESS ROM

$$\dot{(\,)} = \frac{d}{d_\tau}(\,); \psi_k(\xi) = \sin(k\pi\xi)\,; \epsilon_k = \frac{EA}{L_0}\left(\frac{k\pi}{L_0}\right)^2 \frac{A_t}{m_d\left(\tilde{m} + C_a^{pot}\right)\omega_1^2}$$

$$\delta_k = \frac{EI}{m_d\left(\tilde{m} + C_a^{pot}\right)\omega_1^2}\left(\frac{k\pi}{L_0}\right)^4 - \frac{1}{2}\frac{\gamma L_0}{m_d\left(\tilde{m} + C_a^{pot}\right)\omega_1^2}\left(\frac{k\pi}{L_0}\right)^2 + \left(\frac{k\pi}{L_0}\right)^2 \frac{\bar{T}_t}{m_d\left(\tilde{m} + C_a^{pot}\right)\omega_1^2}$$

- Adopted projection functions: $\psi_k(\xi) = \sin(k\pi\xi)$;
- Sensitivity of the results with respect to the choice of the projection functions:

Ongoing research, part of the PhD of Guilherme Vernizzi (see Vernizzi, Franzini & Lenci (2019) – RANM Conference and Vernizzi, Franzini & Lenci (2019) – submitted to Int. J. of Mech. Sciences).

MAPS OF POST-CRITICAL MODAL AMPLITUDES

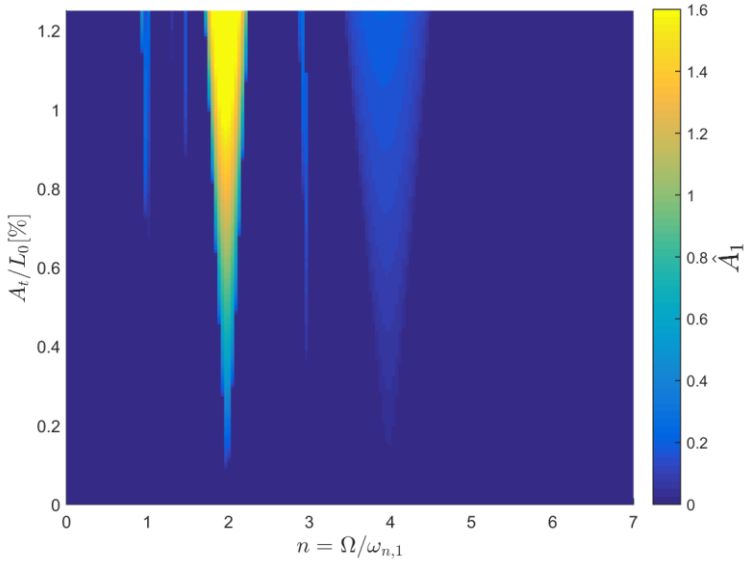

(a) $\hat{A}_1\left({}^{A_t}/_{L_0}, n\right)$

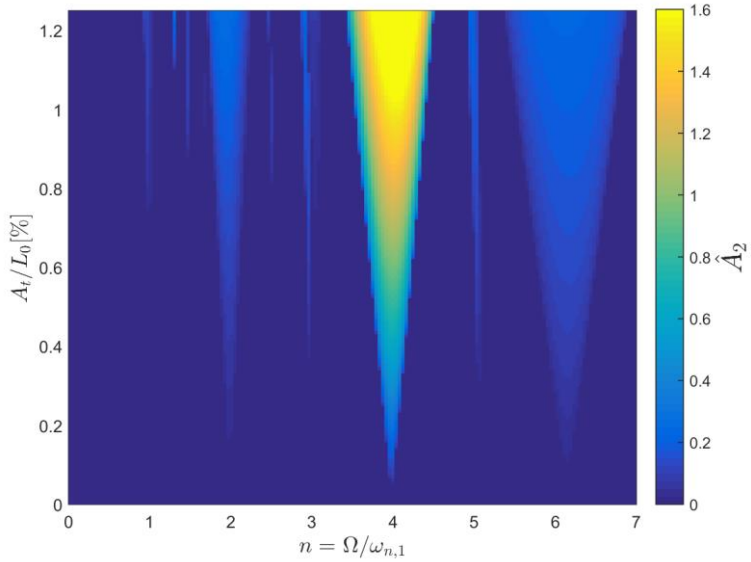

(b) $\hat{A}_2\left({}^{A_t}/_{L_0}, n\right)$

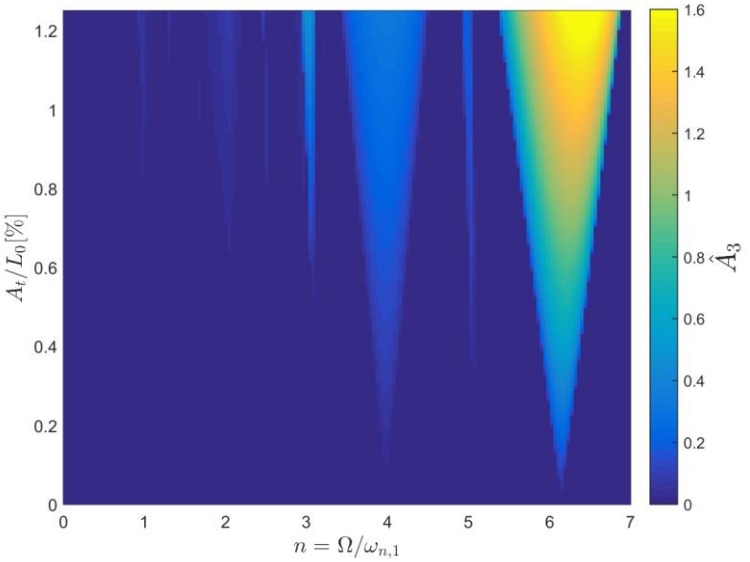

(c) $\hat{A}_3\left({}^{A_t}/_{L_0}, n\right)$

MAPS OF POST-CRITICAL MODAL AMPLITUDES

- Post-critical response maps do not correspond to the Strutt's diagram. They show the characteristic value of the modal-amplitude time-histories as functions of the parameters that govern the parametric excitation;
- The multi-modal character of the ROM allows the appearance of other regions in the plane of control parameter in which lateral responses are observed. This result is not observed if a 1-dof ROM is employed;
- As expected, the parametric excitation frequency associated with the onset of the main region of response corresponds to twice the natural frequency of that mode.

1. General Aspects
2. Experimental analysis of the PE of a flexible and submerged cylinder
3. Mathematical modeling of PE of a vertical and flexible cylinder
4. Passive suppression of PE

PASSIVE SUPPRESSION OF PE

- Rigid cylinder, assembled onto a time-dependent spring support of constant damping;
- Undergraduate research developed by Giovanna Campedelli; results presented in Franzini, Campedelli & Mazzilli (2018), Int. J. of with Non-Linear Mech., v.105, 249-260.
- Part of a research project sponsored by FAPESP – Regular Research Project (2017-2019). Similar studies can be found in the ResearchGate project named ``Passive suppression of oscillations using non-linear vibration absorbers.

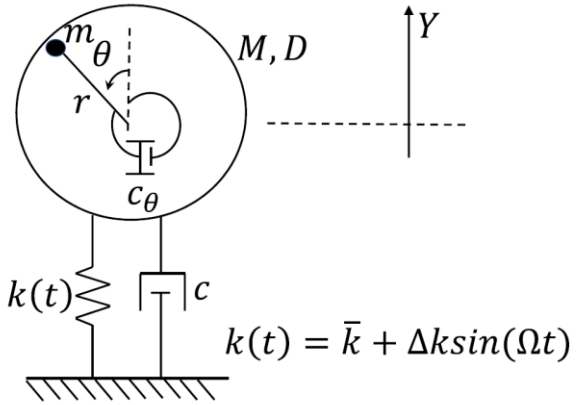

$$\ddot{y} - \beta_1 \sin\theta\ddot{\theta} - \beta_1 \cos\theta\dot{\theta}^2 + \beta_2\dot{y} + (1 + \delta \sin n\tau)y = 0$$

$$\ddot{\theta} - \frac{1}{\hat{r}}\sin\theta\ddot{y} + \beta_3\dot{\theta} = 0$$

$$y = \frac{Y}{D}, \hat{m} = \frac{m}{M}, \hat{r} = \frac{r}{D}, \zeta_y = \frac{c}{2(M+m)\omega_{n,y}}$$

$$\zeta_\theta = \frac{c_\theta}{2mr^2\omega_{n,y}}, \beta_1 = \hat{r}\frac{\hat{m}}{1+\hat{m}}, \beta_2 = 2\zeta_y$$

$$\beta_3 = 2\zeta_\theta, \delta = \frac{\Delta k}{\bar{k}}, n = \frac{\Omega}{\omega_{n,y}}, \tau = \omega_{n,y}t, (\dot{}) = \frac{d()}{d\tau}$$

$$\omega_{n,y} = \sqrt{\frac{\bar{k}}{m+M}}$$

OBJECTIVE

- To check if the rotative NVA is able to suppress the principal parametric instability $(n = 2)$. Gravitational effects are not taken into account;
- To assess the influence of the NVA parameters (mass, *radius* and damping) on the cylinder (main or controlled structure). Similar investigations were not found in the literature;
- Numerical studies; mathematical model numerically, integrated using a Runge-Kutta scheme.
- Initial conditions; $y(0) = 0.1, \theta(0) = {}^{\pi}/_{6}, \dot{y}(0) = \dot{\theta}(0) = 0;$
- The mon-linear character of the mathematical model would lead to important dependence of the response on the initial conditions (possible erosion of the basin of attraction) → Even tough important, this aspect is left for a further work.

MAPS $y_{std}(\hat{m};\hat{r})$

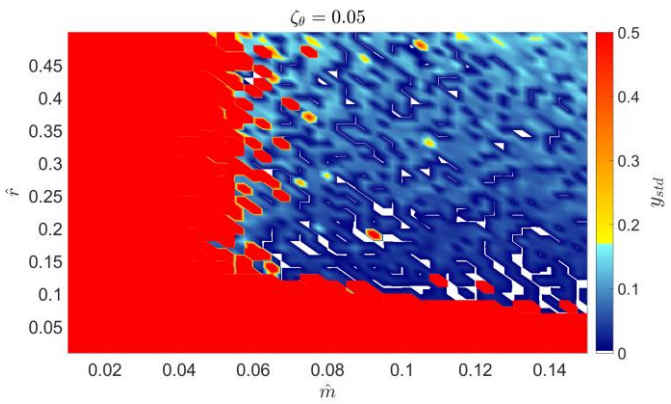

(a) $\zeta_\theta = 0.05$

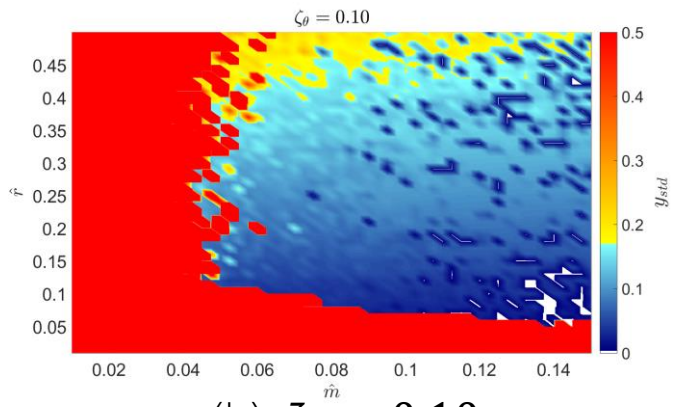

(b) $\zeta_\theta = 0.10$

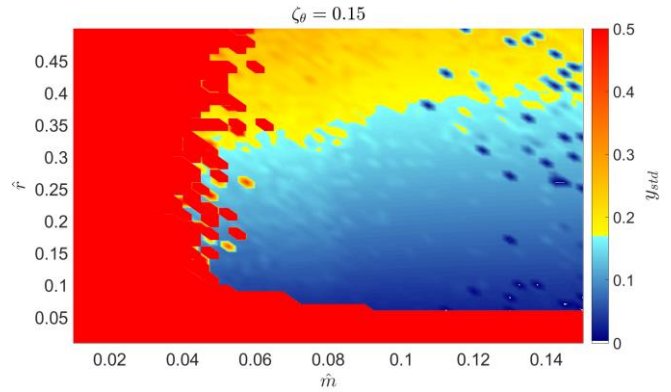

(c) $\zeta_\theta = 0.15$

- Regions shaded in red: unbounded responses (similar to those obtained in the case without the NVA);
- Regions shaded in blue: Small oscillation amplitudes, showing that the NVA is able to limit the structural response even if the parametric excitation frequency leads to the principal parametric instability;
- Erosion of the plane of control parameters is observed, specially for the case with $\zeta_\theta = 0.05$ (regions of unbounded or null oscillatory responses appear inside a region of small responses);
- The increase in ζ_θ enhances the response of the main structure and decreases the erosion of the plane $(\hat{m};\hat{r})$.

A CLOSER INSPECTION

Map $y_{std}(\hat{m};\hat{r})$ and examples of cylinder responses $y(\tau).\zeta_\theta = 0.05$.

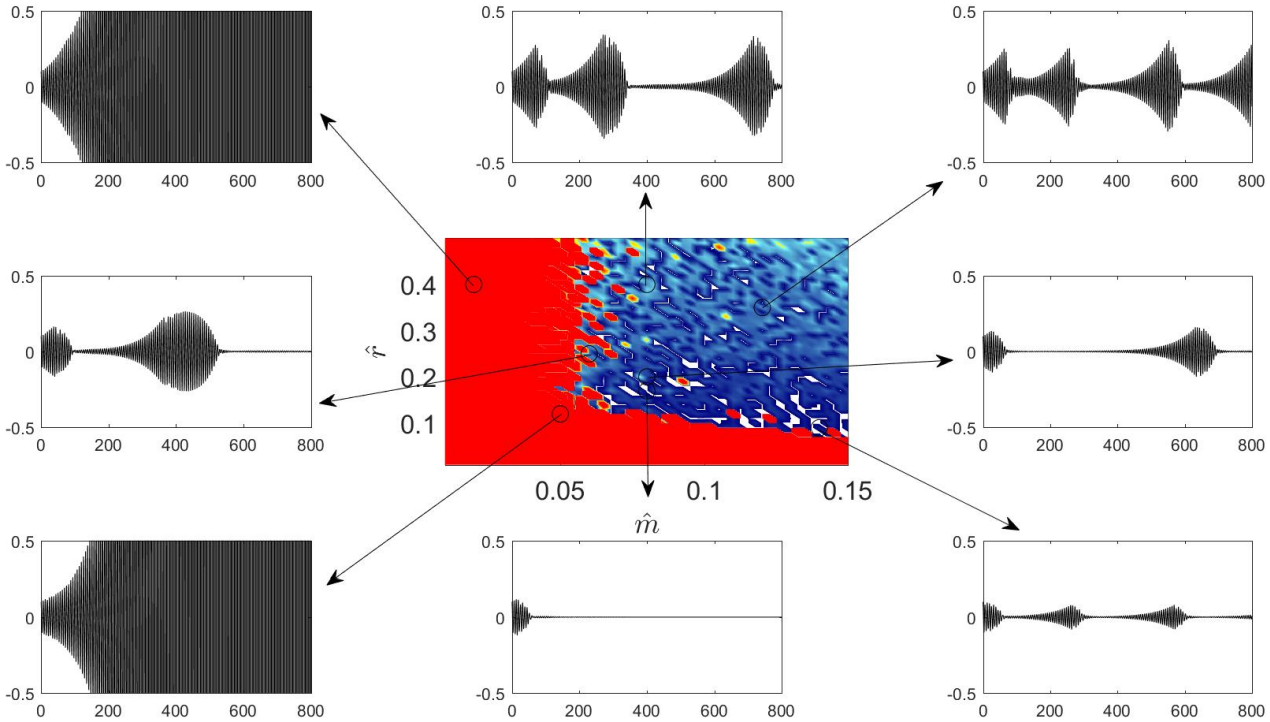

Extracted from Franzini, Campedelli & Mazzilli (2018)

- Different types of responses of the main structure appear: Unbounded solutions, strongly modular responses, complete suppression and steady-state responses (see the paper);
- Besides limiting the cylinder response, the rotative NVA is also able to completely suppress PE (depending on its parameters);

STRONGLY MODULATED RESPONSE

Time-histories and spectral analyses. $\hat{m} = 0.12, \hat{r} = 0.35$ and $\zeta_\theta = 0.05$.

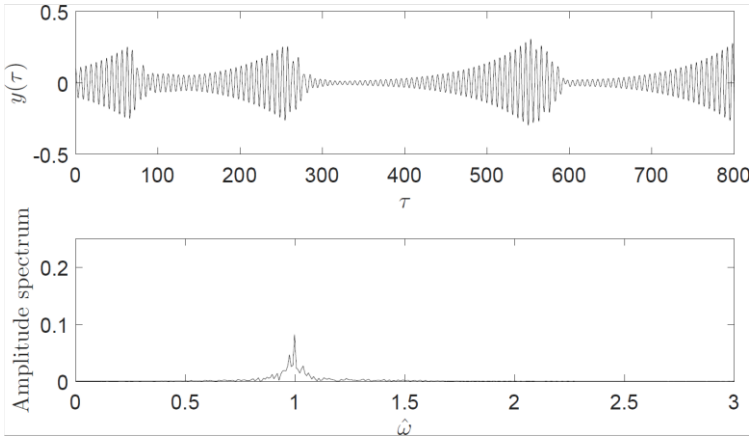

(a) $y(\tau)$

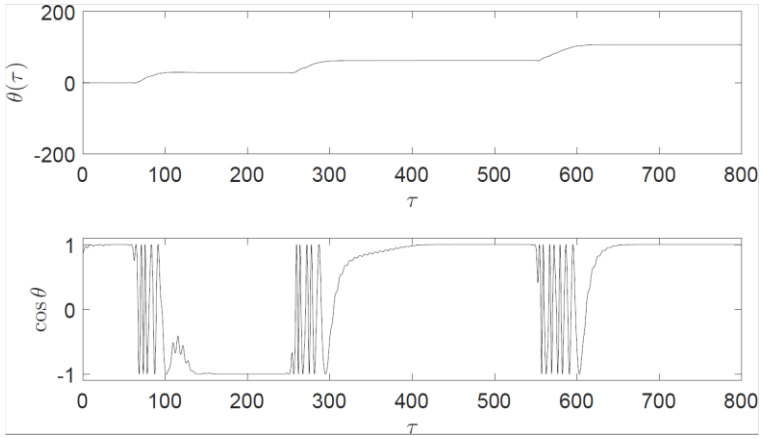

(b) $\theta(\tau)$

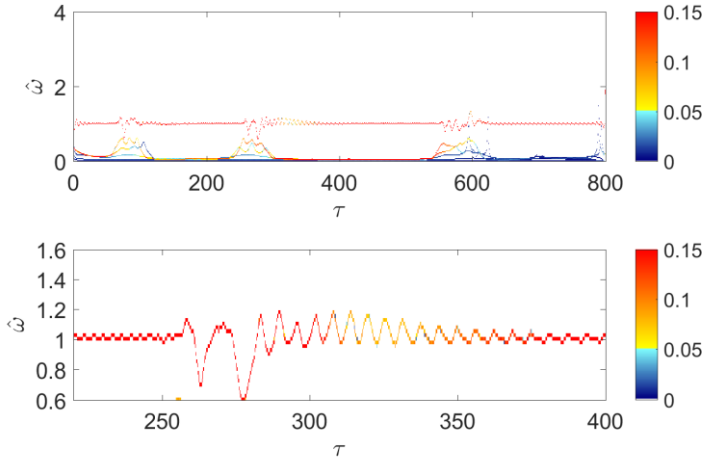

(c) H-H spectrum of $y(\tau)$

Extracted from Franzini, Campedelli & Mazzilli (2018)

STRONGLY MODULATED RESPONSE

- Two distinct response regimes: In the suppression regime, the NVA oscillates with angular velocity practically constant $\boldsymbol{\theta \approx 1}$. In the growing regime, the NVA has no motion $\boldsymbol{(\dot{\theta} \approx \ddot{\theta} \approx 0)}$ and $\boldsymbol{\cos\theta = \pm 1\ (\sin\theta \approx 0);}$
- Growing regime:

$$\ddot{y} - \underbrace{\beta_1 \sin\theta\ddot{\theta} - \beta_1 \cos\theta\dot{\theta}^2}_{\to 0} + \beta_2\dot{y} + (1 + \delta \sin n\tau) = 0, \text{ Damped Mathieu's equation}$$

$$\ddot{\theta} - \underbrace{\sin\theta}_{\to 0}\frac{1}{\hat{r}}\ddot{y} + \beta_3\dot{\theta} = 0, \text{ Trivially satisfied}$$

- An asymptotic perturbation method is employed aiming at investigating the strongly modulated response…

STRONGLY MODULATED RESPONSE – CX-A METHOD

Let us consider the following quantities:

$\beta_1 = \hat{r}\frac{\hat{m}}{1+\hat{m}} = \epsilon, \delta = \epsilon\hat{\delta}, \beta_2 = \epsilon\lambda_2, \ddot{y} = -y + O(\epsilon)$ Assumed

Substituting the above parameters in the equations of motion, one obtains:

$$\ddot{y} + \epsilon\lambda_2\dot{y} + y = \epsilon\left(\sin\theta\ddot{\theta} + \cos\theta\dot{\theta}^2 - \hat{\delta}y\sin n\tau\right)$$

$$\ddot{\theta} + \beta_3\dot{\theta} = -\frac{1}{\hat{r}}\sin\theta y + O(\epsilon)$$

Change of variables (complexification)

$$\phi e^{i\tau} = \dot{y} + iy$$

$$\theta = \tau + \psi$$

STRONGLY MODULATED RESPONSE – CX-A METHOD

After the averaging (similar to the Krylov-Bogoliubov's method)

$$\dot{\phi} + \epsilon\frac{\lambda_2}{2}\,\phi = \frac{\epsilon}{2}\left(-\frac{\hat{\delta}}{2}\phi^* + e^{i\psi}\left[\left(1+\dot{\psi}^2\right) - i\ddot{\psi}\right]\right)$$

$$\ddot{\psi} + \left(1+\dot{\psi}\right)\beta_3 = -\frac{1}{4\hat{r}}\left(\phi^{-i\psi} + \phi^* e^{-i\psi}\right) + O(\epsilon)$$

By applying the method of multiple scales and collecting equations of order ϵ^0, one obtains:

$$D_0\phi_0 = 0 \rightarrow \phi = \phi(\tau_1) = Ne^{i\alpha}; N = N(\tau_1) > 0, \alpha = \alpha(\tau_1)$$

$$D_0^2\psi_0 + \beta_3(1 + D_0\psi_0) = -\frac{1}{4\hat{r}}\left(\phi^{-i\psi_0} + \phi^* e^{i\psi_0}\right)$$

The slow invariant manifold (SIM) is defined as the fixed points of the equations of order ϵ^0.

SIM

$$\cos(\gamma - \alpha) = -\frac{2\beta_3 \hat{r}}{N}$$
$$\gamma = \lim_{\tau_0 \to \infty} \psi_0$$

The investigation of stability of the fixed points allows to point out that the SIM is composed of two branches, one being unstable. The dynamics is observed on the stable branch of the SIM.

Now, we will see an example. Let's assume $\hat{m} = 0.06, \hat{r} = 0.25$ and $\zeta_\theta = 0.15$.

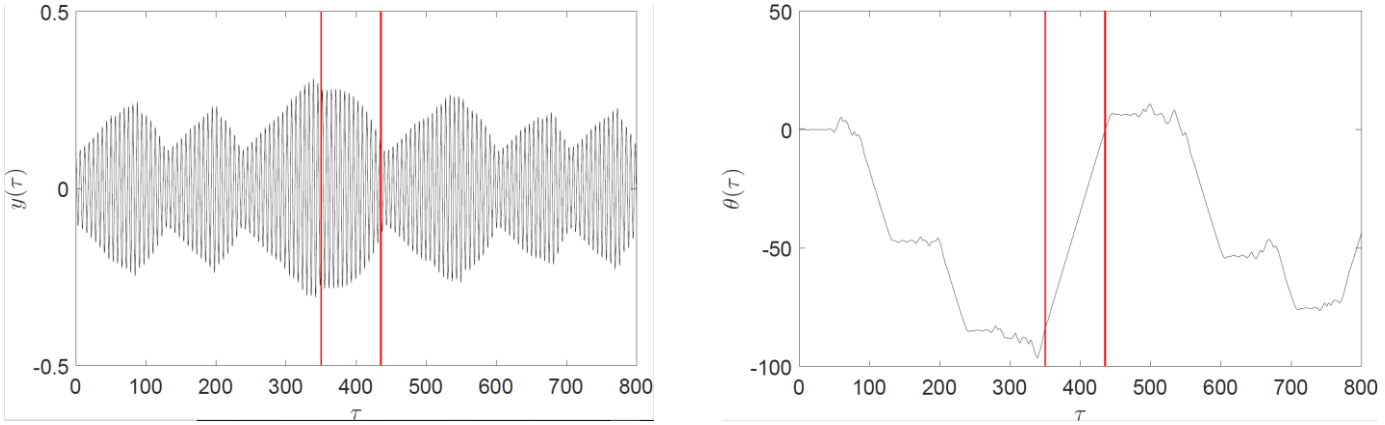

Extracted from Franzini, Campedelli & Mazzilli (2018).

SIM

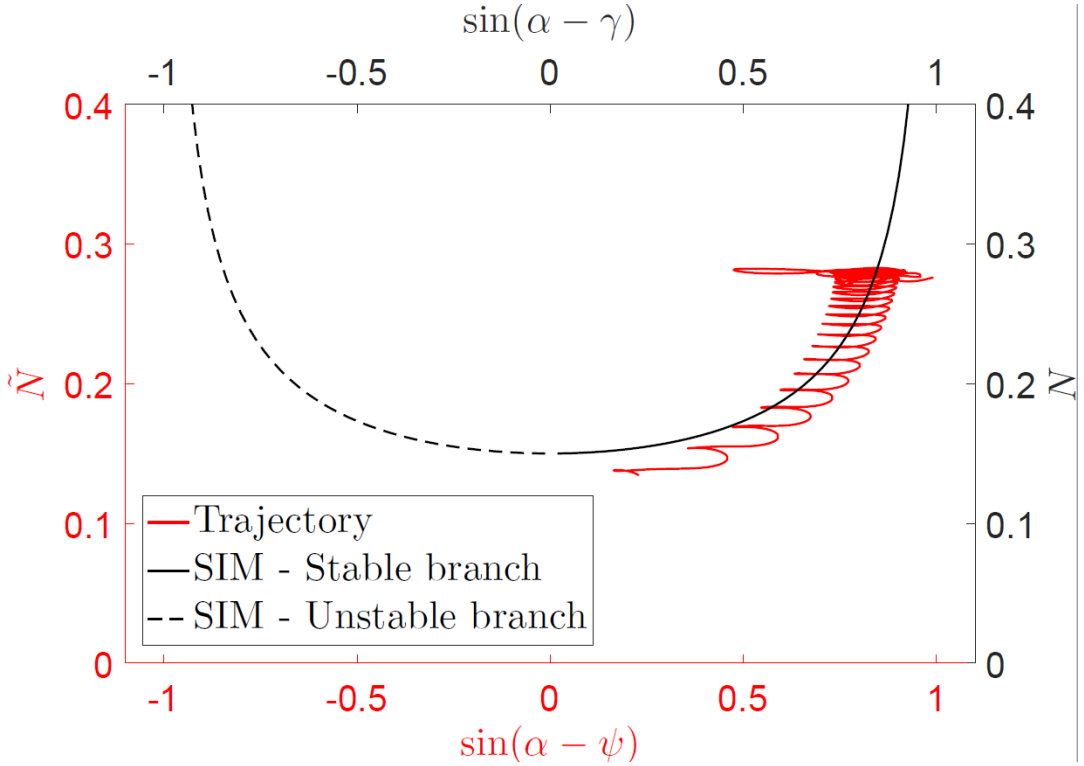

Extracted from Franzini, Campedelli & Mazzilli (2018).

- Qualitative and quantitative agreement between the analytical and the numerical results;
- Strongly modulated response: associated with the capture in a $2:1:1$ resonance (the oscillation frequency is equal to the angular velocity of the NVA, both half the parametric excitation frequency).

SUPPORTING AGENCIES

FAPESP
Grant 2016/20929-2

CNPq
Conselho Nacional de Desenvolvimento Científico e Tecnológico
Grant 310595/2015-0

PETROBRAS

ACKNOWLEDGMENTS

SÃO PAULO SCHOOL OF ADVANCED SCIENCES ON NONLINEAR DYNAMICS

ESCOLA POLITÉCNICA DA UNIVERSIDADE DE SÃO PAULO

PEFUSP

PME Departamento de Engenharia Mecânica

PTC

LMO | Offshore Mechanics Laboratory

FAPESP
Grant 2017/06538-3-2
Giovanna Campedelli

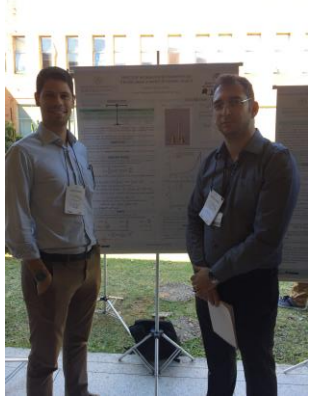

PhD Candidate Giovanni Amaral and master of the PowerPoint

All my ``volunteer'' students that work on the organization

SÃO PAULO SCHOOL OF ADVANCED SCIENCES ON

NONLINEAR DYNAMICS

ESCOLA POLITÉCNICA DA

UNIVERSIDADE DE SÃO PAULO

FAPESP